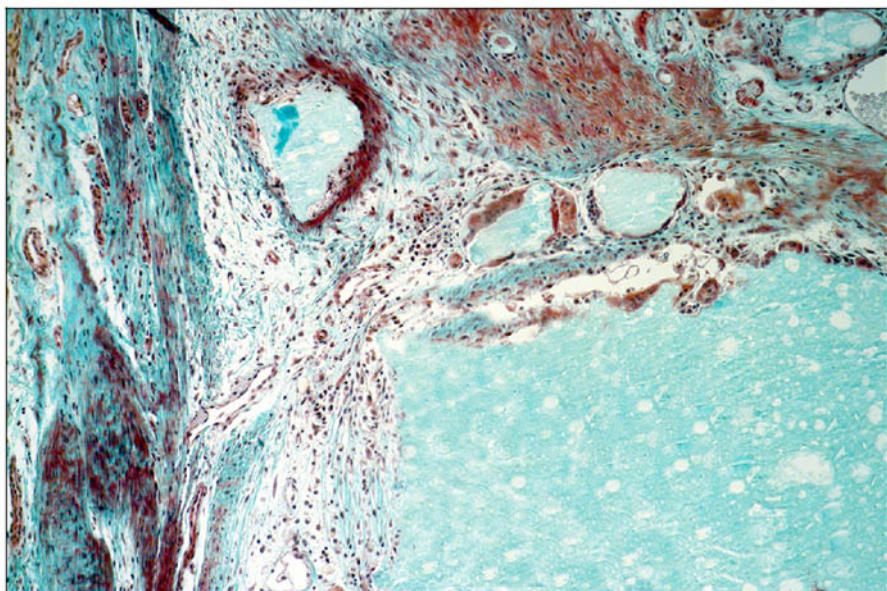


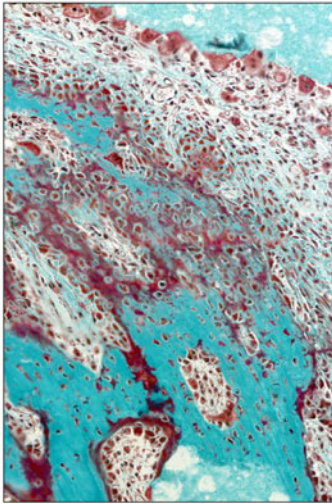
**A. 0.166 mg/mL rhBMP-2/α-BSM**



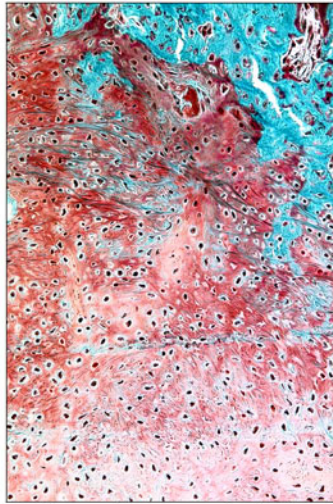
**B. α-BSM**

Fig. E-1

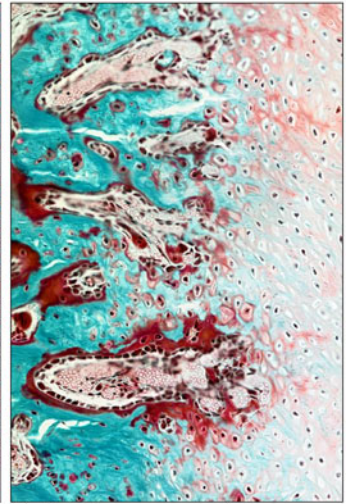
Difference in bone induction at the periphery of a defect in rabbit radii, at four weeks, in response to treatment with 0.166 mg/mL rhBMP-2/α-BSM (A) and α-BSM (B) (Goldner trichrome,  $\times 10$ ). Rapid induction of new bone adjacent to the soft tissue is apparent at the periphery of the defect treated with rhBMP-2/α-BSM (A). In contrast, there was no evidence of bone formation at the periphery of the defect treated with α-BSM (B).



**A. Direct bone formation**



**B. Fibrocartilage conversion to bone**

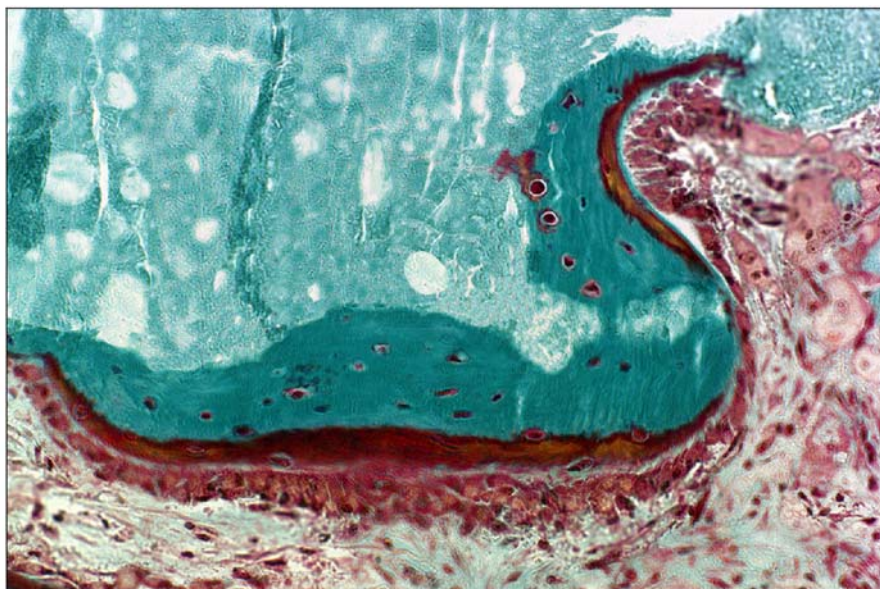


**C. Cartilage conversion to bone**

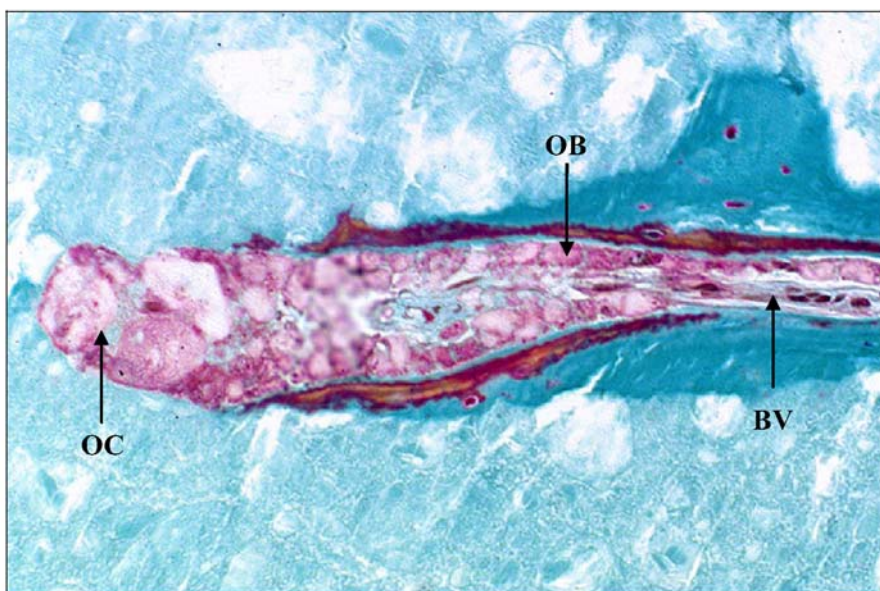
Fig. E-2

Mechanisms of bone formation within rabbit radius defects at four weeks (Goldner trichrome,  $\times 20$ ). Direct woven bone formation in association with neovascularization either on  $\alpha$ -BSM granules or adjacent to resorbing  $\alpha$ -BSM granules predominated at four weeks within the defects treated with 0.166 mg/mL rhBMP-2/ $\alpha$ -BSM (A). Occasionally, a small area of bone induction involving sequential conversion of cartilage to fibrocartilage and then to bone was observed in the rhBMP-2/ $\alpha$ -BSM groups (B). Regions of more typical endochondral conversion of cartilage to bone were more often noted near the ends of the defects in the  $\alpha$ -BSM-treated rabbits (C).





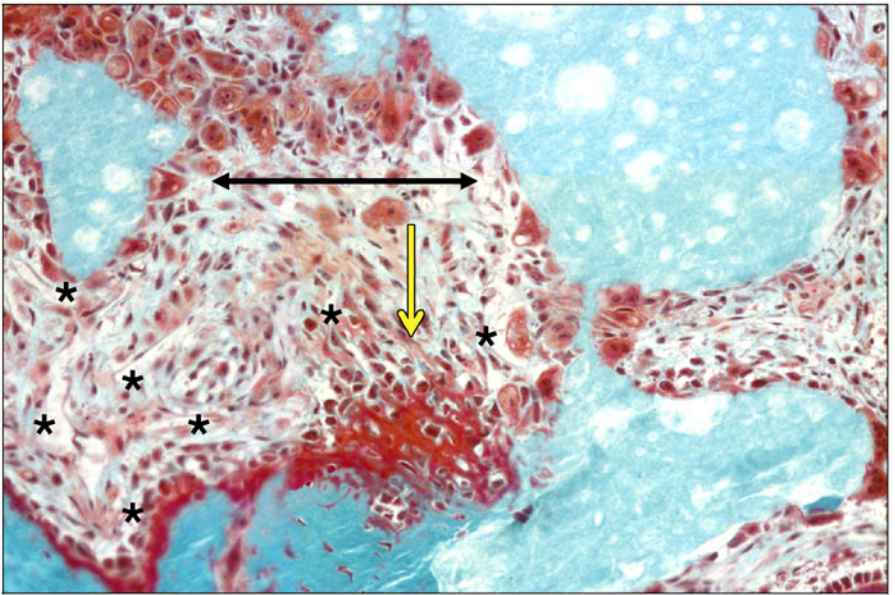
**A. Appositional bone formation on  $\alpha$ -BSM granules**



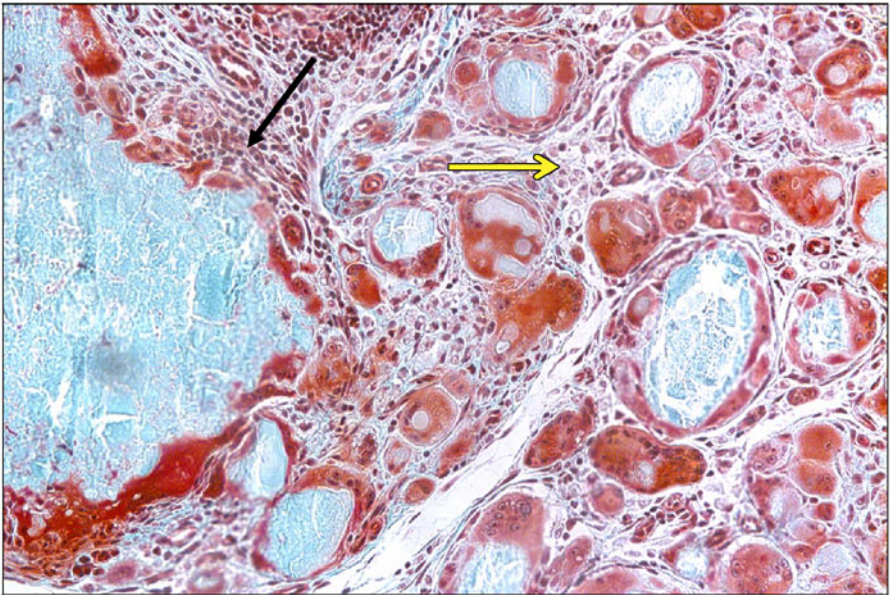
**B. Bone formation within  $\alpha$ -BSM granules generated by cutting cones**

Fig. E-3

Appositional and osteonal bone formation in association with  $\alpha$ -BSM granules within a defect in a rabbit radius treated with 0.166 mg/mL rhBMP-2/ $\alpha$ -BSM (Goldner trichrome,  $\times 20$ ). Appositional bone formation directly on  $\alpha$ -BSM granules (A) was observed in all of the treatment groups. Remodeling cutting cones containing osteoclasts (OC), osteoblasts (OB), and blood vessels (BV) created osteons of newly formed bone within the  $\alpha$ -BSM granules (B) in all of the treatment groups.



**A. 0.033 mg/mL rhBMP-2/α-BSM**

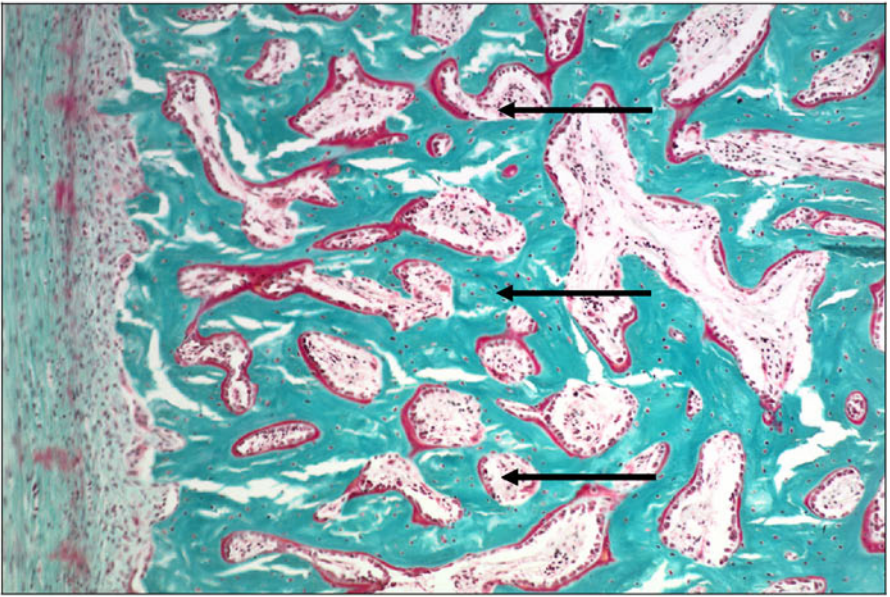


**B. α-BSM**

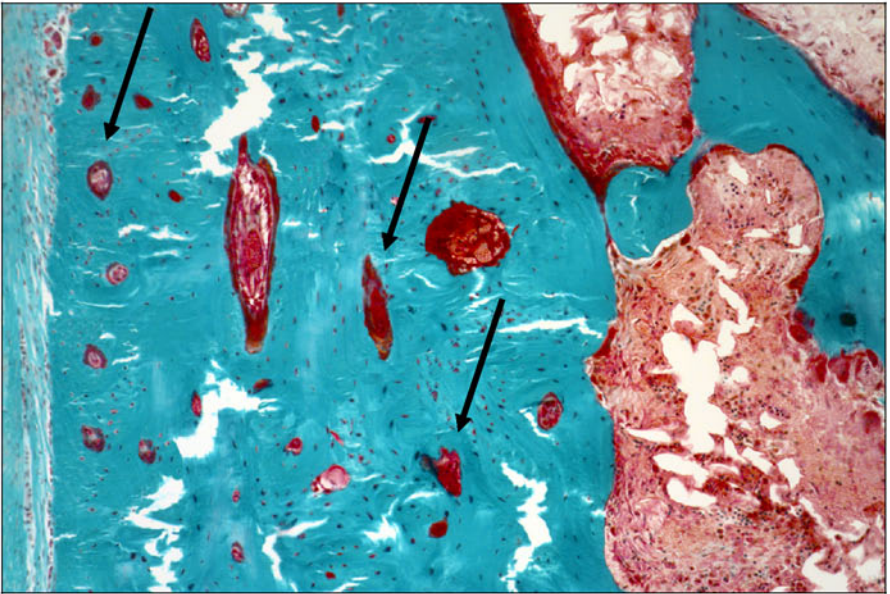
Fig. E-4

Resorption of α-BSM in a rabbit radial defect treated with 0.033 mg/mL rhBMP-2/α-BSM (A) compared with that in a defect treated with α-BSM (B) (Goldner trichrome, ×20). Resorption of α-BSM by osteoclasts (black arrows) predominated in the rhBMP-2/α-BSM-treated defects (A). Giant cells were occasionally observed resorbing small granules of α-BSM. Rapid bone induction (yellow arrow) and neovascularization (★) were observed in response to rhBMP-2 released from the resorbing α-BSM (A). Resorption of α-BSM by a combination of osteoclasts (black arrow) and giant cells (yellow arrow) was observed in the α-BSM-treated defects (B).





**A. 0.166 mg/mL rhBMP-2/ $\alpha$ -BSM group (4 weeks)**



**B. 0.166 mg/mL rhBMP-2/ $\alpha$ -BSM group (8 weeks)**

Fig. E-5

Regeneration of the cortex in rabbit radial defects at four (A) and eight (B) weeks after treatment with 0.166 mg/mL rhBMP-2/ $\alpha$ -BSM (Goldner trichrome,  $\times 10$ ). Accelerated appositional bone formation on newly formed trabeculae at the periphery of the defect initiates the process of cortical regeneration at four weeks by filling in the spaces between adjacent trabeculae (A, arrows). Continued peripheral appositional bone formation and osteonal remodeling of the consolidated trabecular bone result in regeneration of the cortex at eight weeks (B, arrows). The process of corticalization is associated with neovascularization.